International Journal of Minerals, Metallurgy and Materials
Volume 22, Number 12, December 2015, Page 1252
DOI: 10.1007/s12613-015-1192-x

Coordinated control of carbon and oxygen for ultra-low-carbon interstitial-free steel in a smelting process

Min Wang[1,2)], *Yan-ping Bao*[1)], *Quan Yang*[2)], *Li-hua Zhao*[1)], *and Lu Lin*[1)]

1) State Key Laboratory of Advanced Metallurgy, University of Science and Technology Beijing, Beijing 100083, China

2) National Engineering Research Center of Flat Rolling Equipment, University of Science and Technology Beijing, Beijing 100083, China

(Received: 22 December 2014; revised: 12 March 2015; accepted: 17 March 2015)

Abstract: Low residual-free-oxygen before final de-oxidation was beneficial to improving the cleanness of ultra-low-carbon steel. For ultra-low-carbon steel production, the coordinated control of carbon and oxygen is a precondition for achieving low residual oxygen during the Ruhrstahl Heraeus (RH) decarburization process. In this work, we studied the coordinated control of carbon and oxygen for ultra-low-carbon steel during the basic oxygen furnace (BOF) endpoint and RH process using data statistics, multiple linear regressions, and thermodynamics computations. The results showed that the aluminum yield decreased linearly with increasing residual oxygen in liquid steel. When the mass ratio of free oxygen and carbon ([O]/[C]) in liquid steel before RH decarburization was maintained between 1.5 and 2.0 and the carbon range was from 0.030wt% to 0.040wt%, the residual oxygen after RH natural decarburization was low and easily controlled. To satisfy the requirement for RH decarburization, the carbon and free oxygen at the BOF endpoint should be controlled to be between 297×10^{-6} and 400×10^{-6} and between 574×10^{-6} and 775×10^{-6}, respectively, with a temperature of 1695 to 1715°C and a furnace campaign of 1000 to 5000 heats.

Keywords: low carbon steel; smelting; decarburization; cleanness

1. Introduction

The main functions of a basic oxygen furnace (BOF) are decarburization and dephosphorization by oxygen injection from the top lance [1]. During the BOF smelting process, elements C, Fe, Si, Mn, and Ti in liquid steel, along with heterogeneous slag with gas bubbles and solid materials, participate in reactions; thus, the BOF smelting process is highly complicated. Good BOF endpoint control is necessary and important for clean steel production [2−4]. Maintaining a high hit rate at the BOF endpoint on the sole basis of operator judgment is difficult; automated control has therefore gradually become a trend. At present, BOF endpoint control methods are based primarily on sublance technology, the real-time measurement of off-gas composition, or both [5−7]. BOF endpoint hit rates that include the carbon and phosphorus contents and the temperature have been successfully predicted on the basis of sublance or off-gas composition measurement results and dynamic control models (e.g., neural network models, multiple regression models, self-learning models, etc.) [8−10]. In fact, sublance or real-time measurements of off-gas composition combined with dynamic control models enable the precise prediction of BOF endpoint. Thus, the determination of reasonable conditions such as temperature and carbon/oxygen contents has become another key point for the production of high-quality steel. Good conditions at the BOF endpoint can guarantee control during the next stage and steel cleanness [11−12]. Ultra-low-carbon interstitial-free steel (IF steel) is widely used in the automobile and appliance industries; because of the low carbon ($< 20 \times 10^{-6}$) and nitrogen ($< 30 \times 10^{-6}$) contents of the steel, the carbon and nitrogen contents are strictly controlled during the whole steelmaking process. Control of the conditions related to the BOF endpoint and RH treatment, such as the temperature of liquid steel and its carbon and free oxygen contents, are extremely important for minimizing production

Corresponding author: Min Wang E-mail: worldmind@163.com

costs and maximizing steel quality.

2. Experimental method and process

In this paper, we focused on the coordinated control of carbon and oxygen during the BOF and RH process for the production of IF steel. The target chemical composition is listed in Table 1. The experiments were performed at Shougang Qian'An Iron & Steel Works. The production process is described as follows: 210-t BOF → RH decarburization → Al-killed and Ti stabilized → 60-t tundish → 1200 mm × 210 mm continuous casting slab.

Table 1. Target chemical composition of steel grade A wt%

[C]	[Si]	[Mn]	[P]	[S]	$[Al]_T$	[Ti]	[N]
≤ 0.002	≤ 0.020	0.130	≤ 0.009	≤ 0.010	0.030	0.070	≤ 0.004

To obtain reasonable process control conditions for the BOF endpoint and RH treatment, 590 heats process data were recorded over a period of 12 consecutive months. The BOF data included hot-metal information (including temperature, composition, adding time, etc.), smelting information (including furnace campaign, heat number, oxygen blowing pressure and flow, blowing time, scrap amount, etc.), and endpoint information (including compositions of the liquid steel at different times, free oxygen content, temperature, sampling time, etc.). RH data included information about the liquid steel (including composition, temperature, free oxygen content before and after RH decarburization, etc.), and RH refining information (including weight of the liquid steel, alloy weight and addition time for de-oxidation and alloying, vacuum time and circulation time, oxygen blowing amount, etc.).

First, the data were sorted according to the heat number. Second, incomplete heat data were filtered and removed. Here, incomplete heat data refers to heats where three or more of the aforementioned data points were missed in the same heat. After data filtering, 489 heats with complete data remained. On the basis of process data analysis, reasonable process control conditions for ultra-low-carbon steel production in a 210-t BOF and RH system are summarized. Finally, a verification experiment was performed using the optimized conditions.

3. Results and discussion

3.1. Coordinated control of carbon and oxygen in the BOF process

The product of carbon content and free oxygen content in liquid steel ([C]·[O] product) can be used to evaluate the status of the equilibrium. We divided the data for the 489 heats into different groups according to temperature and BOF furnace campaign sequences to investigate the average change in [C]·[O] product at the BOF endpoint and to compare the relationship between the average [C]·[O] product and the temperature or furnace campaign at the BOF endpoint.

Fig. 1 shows the relationship between the average [C]·[O] product and temperature. Here, the 489 heats were divided into six groups according to the change in temperature. The temperature ranges in the first and last groups are below 1695°C and above 1735 °C, respectively; 17 and 54 heats were categorized into the first and last groups, respectively. Between the first and last groups, the temperature interval is 10°C.

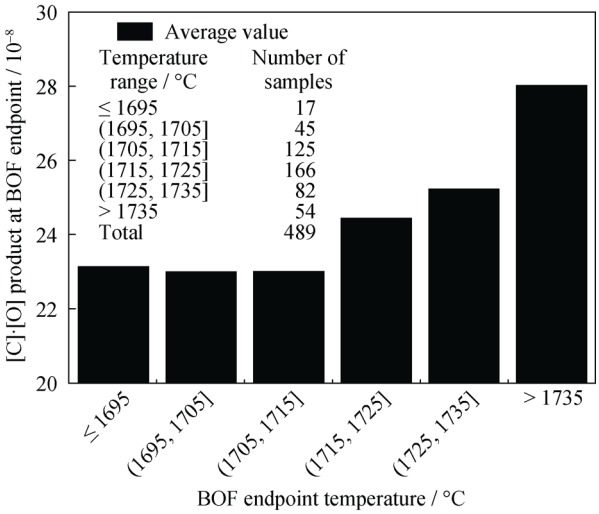

Fig. 1. Relationship between [C]·[O] product and temperature at the BOF endpoint (the *x*-coordinate value (*a*, *b*] represents the temperature range between value *a* and value *b* but not including *a*).

As shown in Fig. 1, when the BOF endpoint temperature exceeds 1715°C, the average value of the [C]·[O] product increases significantly. When the target carbon content in liquid steel is fixed, a high [C]·[O] product value indicates a large amount of free oxygen exists in liquid steel. Maintaining the temperature between 1695 and 1715°C is beneficial for the control of low free oxygen. In this range, the average [C]·[O] product is 23×10^{-8}. When the temperature is below the low limit value (1695°C), the chemical heating process induced by adding aluminum and injecting oxygen into the liquid steel from the top lance during the RH process becomes necessary; this process prolongs the RH treatment time and adversely affects steel cleanness. Temperatures that exceed the upper limit result in high free oxygen con-

tent in the liquid steel after decarburization because of over-oxidation of the liquid steel.

Fig. 2 shows the relationship between the average [C]·[O] product and the BOF furnace campaign. Seven groups are established according to the furnace campaign. The average [C]·[O] product increases gradually as the furnace campaign progresses. This increase in the average [C]·[O] product promotes reaction equilibrium in the liquid steel because argon and oxygen are injected from the bottom and top, respectively, during the BOF process. However, in the BOF post-campaign regime (> 5000 heats), gas permeability at the bottom blowing holes decreases, the over-oxidation of the liquid steel increases, and the [C]·[O] product increases significantly. A stable [C]·[O] product range is 22×10^{-8} to 24×10^{-8} with furnace campaign between 1000–5000 heats.

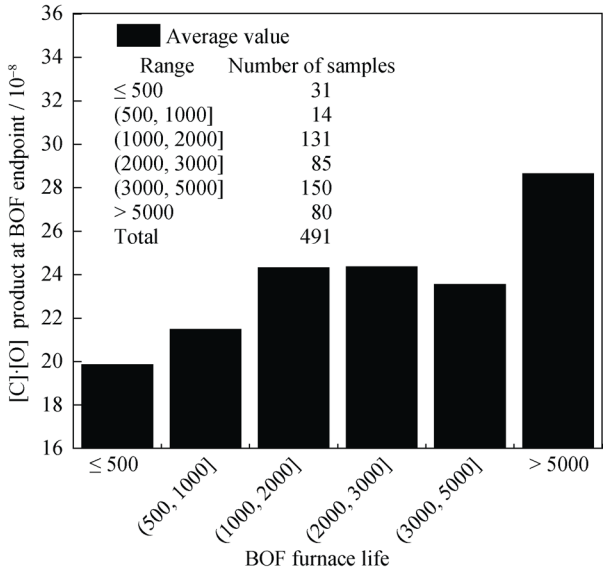

Fig. 2. Relationship between [C]·[O] product and BOF furnace campaign (the *x*-coordinate value (*a*, *b*] represent furnace campaign range between value *a* and value *b* but not including *a*).

The [C]·[O] product in liquid steel could be calculated by the following equations:

$$[C]+[O]=CO_{(g)} \tag{1}$$

$$\lg K = 1160/T + 2.003 \tag{2}$$

$$[C]\cdot[O] = \frac{P_{CO}}{K}\cdot\frac{1}{f_C \cdot f_O} \tag{3}$$

$$\lg f_i = \sum e_i^j \cdot w_{[j]} \tag{4}$$

where P_{CO} represents the partial pressure of CO in the gas atmosphere ($P_{CO} + P_{CO2} = 1$); [C] and [O] represent the contents of carbon and soluble oxygen in the liquid steel; $f_{[C]}$ and $f_{[O]}$ represent the activity coefficients of the carbon and oxygen, respectively, in liquid steel; T (K) is the temperature; and K is the equilibrium constant of reaction (1); e_i^j represents the interaction coefficients of element j to the element i. The [C]·[O] product varied with the chemical composition of the liquid steel, the temperature, and the partial pressure of carbon monoxide (P_{CO}), as mentioned in Eqs. (3) and (4).

We can estimate the theoretical [C]·[O] product in liquid steel under different conditions with above equations. When the carbon content is high, P_{CO} tends to approach 1. Generally, the partial pressure of CO (P_{CO}) ranges between 0.8 and 1.0 [13]; however, it decreases to less than 1 during the production of ultra-low carbon steel because of its over-oxidation at the BOF endpoint; here, the range of P_{CO} is set as 0.7 to 1.0; f_C and f_O are calculated according to Eq. (4) on the basis of the data in Tables 2 and 3. The value ranges are f_C = 0.90–0.98 and f_O = 0.86–0.98; therefore, the range of (f_C:f_O) is 0.78–0.96; we set the f_C:f_O to be 0.9. The theoretical lines of carbon and free oxygen contents under different conditions and the scatters of real values are described in Fig. 3.

Table 2. Chemical composition range of grade A at BOF endpoint wt%

[C]	[Si]	[Mn]	[P]	[S]	[O]
0.010–0.080	≤ 0.010	0.130	≤ 0.009	≤ 0.010	0.035–0.200

Table 3. Interaction coefficients of elements

e_i^j	C	Si	Mn	P	S	O
C	0.243	0.08	−0.0084	0.051	0.044	−0.32
O	−0.421	−0.066	−0.021	0.07	−0.133	−0.17

Fig. 3 shows that the partial pressure of carbon monoxide affects the [C]·[O] product more significantly than does temperature. When the temperature increased by 20°C with the same partial pressure of carbon monoxide and the same carbon content, the oxygen content increased by 20×10^{-6}; however, when the partial pressure of carbon monoxide (P_{CO}) changed from 1.0 to 0.7, the free oxygen content decreased by 200×10^{-6} with a carbon content of 0.030wt%. When the carbon content exceeded 0.035wt%, the measured values were close to the equilibrium line (P_{CO} = 1.0 and T = 1715°C). When the carbon content was lower than 0.035wt%, the measured values shifted toward the equilibrium line (P_{CO} = 0.7 and T = 1715°C); these results indicate that the P_{CO} decreases and CO_2 is formed because of the reaction ($2CO(g) + O_2(g) = 2CO_2(g)$) during this process. Thus, when the carbon in the liquid steel decreases to a critical

value, not all of the oxygen blown into the liquid steel is used for decarburization; some reacts with the CO gas present in the system, and some reacts with Fe in the liquid steel. These processes are easily verified by the selective oxidation between [C] and [Fe] according to Eqs. (5) and (6),

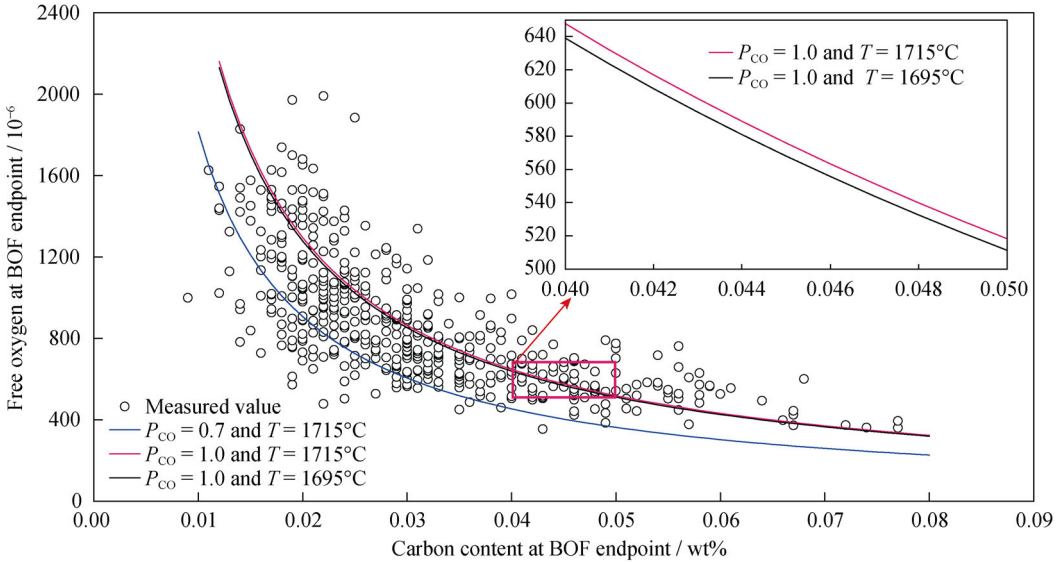

Fig. 3. Comparison between the measured and calculated values of the carbon and oxygen contents in liquid steel.

$$(\mathrm{FeO})+[\mathrm{C}]=[\mathrm{Fe}]+\mathrm{CO}_{(g)},\quad \Delta G^{\ominus}=99000-90.72T \tag{5}$$

$$\Delta G=\Delta G^{\ominus}+RT\ln\left(\frac{P_{\mathrm{CO}}}{[\mathrm{C}]\cdot a_{(\mathrm{FeO})}}\cdot\frac{1}{f_{[\mathrm{C}]}}\right) \tag{6}$$

where $\Delta G^{\ominus}$ is the standard Gibbs free energy of reaction; ΔG represents the Gibbs free energy of reaction; R is the ideal gas constant (8.314 J·mol^{-1}·K^{-1}); and $a_{(\mathrm{FeO})}$ represents the activity of FeO in the BOF slag (here, the value range is set to 0.35 [14]).

As shown in Fig. 4, the critical carbon content of selective oxidation decreases with increasing temperature. Under 1650°C, the oxygen being blown into liquid steel preferentially reacts with Fe when the carbon content is less than 0.025wt%. According to the results in Figs. 3 and 4, the carbon content should be controlled to be between 250 × 10^{-6} and 450 × 10^{-6} at the BOF endpoint. When the carbon content is within this range, reaction (1) is close to equilibrium, the free oxygen content is reasonable, and the extent of over-oxidation is low.

On the basis of the aforementioned analysis, the conditions at the BOF endpoint necessary to make the [C]·[O] product shift toward the equilibrium line are summarized as follows. (1) The BOF furnace campaign should be within 1000–5000 heats during ultra-low-carbon steel production because the [C]·[O] product increases significantly and diverges from the equilibrium line when the furnace campaign heats exceed 5000. (2) The carbon content at the BOF endpoint should be controlled to be between 250 × 10^{-6} and 450 × 10^{-6}. When the carbon content is less than 250 × 10^{-6}, the free oxygen content increases and the liquid steel becomes over-oxidation; when the carbon content exceeds 450 × 10^{-6}, the conditions required for decarburization during the RH process cannot be achieved. (3) The BOF endpoint temperature should be between 1695 and 1715°C because the

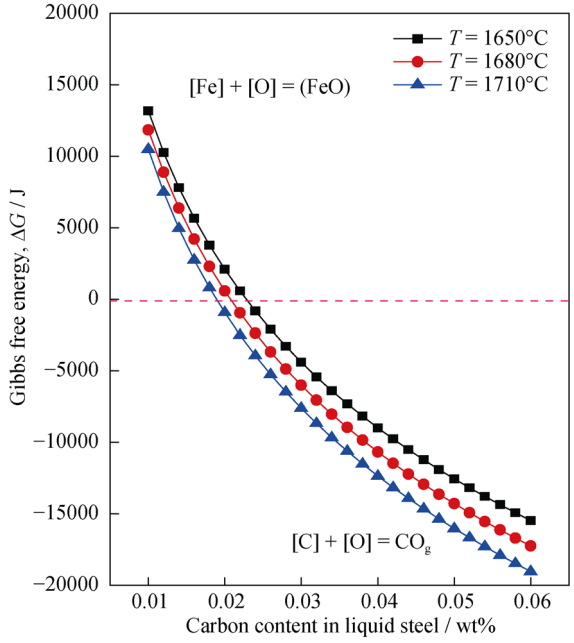

Fig. 4. Selective oxidation between [C] and [Fe] during oxygen blowing.

[C]·[O] product increases significantly at temperatures above 1715°C. These conditions are narrowed and confirmed further in the next section on the basis of other data.

The increase in temperature per 0.01wt% reduction of carbon in liquid steel during the re-blowing process can be calculated by Eq. (7); and the data are described in Fig. 5.

$$\eta = \Delta T / \Delta C = \frac{(T_2 - T_1)}{(w_{C_1} - w_{C_2})} \cdot \frac{1}{100} \tag{7}$$

Here, η represents the increase in temperature per 0.01wt% reduction of carbon in liquid steel during the re-blowing process; T_1 and T_2 represent the temperature of first-catch carbon and BOF endpoint, °C; and w_{C_1} and w_{C_2} represent the carbon contents of first-catch and BOF endpoint in the liquid steel, respectively.

As shown in Fig. 5, when the first-catch carbon content is lower than 0.3wt%, the increasing rate of the temperature increases significantly during oxygen injection for catching the carbon content of BOF endpoint, which will result in high temperature and over-oxidation of liquid steel at BOF endpoint. The relationship between η and the first-catch carbon content in liquid steel during the BOF process was regressed on the basis of measured values:

$$\eta = 1.52 + 132481.34 / \{1 + \exp[(x + 0.94) / 0.11]\} \tag{8}$$

where x represents the carbon content of the first-catch in liquid steel. The R^2 value for this regression was 0.81.

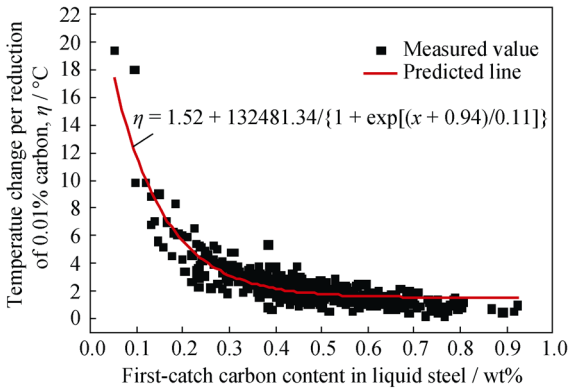

Fig. 5. Relationship between temperature change per 0.01wt% reduction of carbon (η) and first-catch carbon content in liquid steel during the BOF process.

Stable and precise control of the carbon content and temperature at the BOF endpoint can be attained through control of the first-catch carbon to a reasonable level. For example, if the target carbon content and target temperature at the BOF endpoint are 0.040wt% and 1710°C, respectively, then the first-catch carbon content and temperature should be controlled in the ranges from 0.3wt% to 0.4wt% and 1602 to 1658°C, respectively, based on the data in Table 4. A narrower first-catch carbon range enables easier control of the target carbon and target temperature at the BOF endpoint.

Table 4. Range of first-catch carbon content and η value

Range of first catch carbon content / wt%	0.1–0.2	0.2–0.3	0.3–0.4	0.4–0.8
Range of η value	6.0–11.0	3.0–6.0	2.0–3.0	1.5–2.0

3.2. Coordinated control of carbon and oxygen during the RH process

The liquid steel enters the RH refining process after BOF tapping. The RH treatment process features two main tasks: reduce the carbon content to less than 20×10^{-6} by RH decarburization, and ensure low residual-free oxygen content after decarburization. Two different RH decarburization modes (natural decarburization and forced decarburization) for IF steel were adopted in this work. Under the natural decarburization mode, the mass ratio of carbon and oxygen is less than 0.75; the free oxygen is sufficient to satisfy the requirements of decarburization. The carbon and oxygen content ranges should be maintained to satisfy the requirements of natural decarburization and ensure low residual-free oxygen content after decarburization; otherwise, high residual-free oxygen content will result in more inclusions after de-oxidation. Under forced decarburization mode, the mass ratio of carbon and free oxygen in liquid steel is greater than 0.75, which indicates that the free oxygen content does not satisfy the requirement of decarburization; more oxygen is blown into the liquid steel from the top lance of the RH system for decarburization, which also results in an increase in the free oxygen content after decarburization. Thus, coordinated control of the carbon and oxygen contents during the RH process is very important for steel cleanness [15−17]. The amount of inclusions is related to the final residual oxygen content after decarburization. After aluminum is added, a portion of the aluminum is used to react with soluble oxygen, and another portion of the aluminum becomes soluble aluminum. The yield rate of aluminum is calculated according to the following equation:

$$\gamma_{Al} = \frac{\left([Al]_s - [Al]_s^0\right) \cdot W_{Steel}}{W_{Al}} \times 100\% \tag{9}$$

where γ_{Al} is the yield rate of aluminum; $[Al]_s^0$ and $[Al]_s$ are the contents of acid-soluble aluminum before the aluminum addition and at the end of the RH process, respectively; W_{Steel} and W_{Al} are the mass of liquid steel and the mass of the aluminum added to the liquid steel, respectively,

kg. Before the aluminum addition, the content of soluble aluminum ($[Al]_s^0$) approaches to 0.

Fig. 6 shows the relationship between the aluminum yield rate and the residual-free oxygen content in liquid steel under natural decarburization. Among the 489 heats, 327 heats involved natural decarburization and 162 heats involved forced decarburization. Data from the natural decarburization mode based on calculation of Eq. (9) are shown in Fig. 6. The aluminum yield rate decreased linearly with increasing residual-free oxygen content in liquid steel after decarburization; when the oxygen content after decarburization was less than 300×10^{-6}, the aluminum yield rate reached approximately 40%. The yield rate was less than 15% when the residual oxygen content exceeded 600×10^{-6}. The low aluminum yield rate meant that most of the aluminum reacted with oxygen because of the high residual oxygen content after decarburization, resulting in the formation of abundant Al_2O_3 inclusions. Thus, to satisfy the requirement of steel cleanness, the target carbon and free oxygen should be $< 20 \times 10^{-6}$ and $< 400 \times 10^{-6}$, respectively, after RH decarburization.

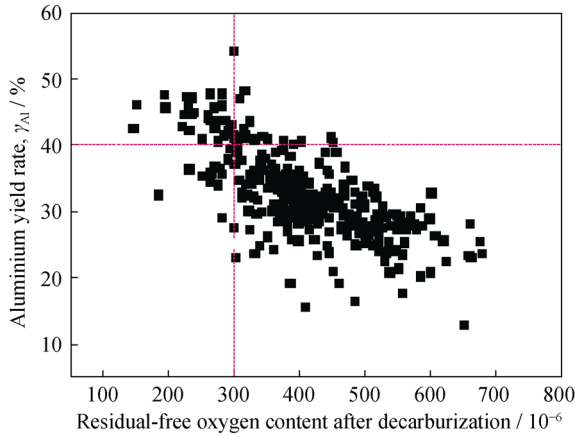

Fig. 6. Relationship between aluminum yield rate and residual-free oxygen content in liquid steel after decarburization under natural decarburization.

Fig. 7 shows the relationship between the carbon content ([C]) and free oxygen content ([O]) in liquid steel before RH decarburization. In region A, the free oxygen content is sufficient to satisfy the requirement for natural decarburization. After decarburization, a large amount of residual oxygen remains, which results in increased aluminum consumption. In region B, free oxygen in the liquid steel cannot satisfy the requirement for RH decarburization. Extra oxygen is blown into the liquid steel from the top lance of the RH system to induce forced decarburization; in fact, more than 95% of the heats in region A involved natural decarburization and more than 85% of the heats in region B involved forced decarburization. The amount of oxygen blown into the liquid steel was between 20 and 300 m^3, depending on the [O]/[C] mass ratio before decarburization. On the basis of the aforementioned analysis, reasonable carbon and free oxygen regions before decarburization should be 0.030wt% to 0.040wt% and 500×10^{-6} to 700×10^{-6}, respectively.

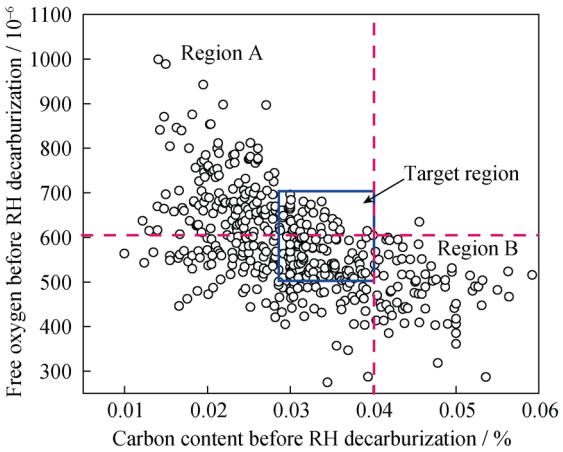

Fig. 7. Relationship between [C] and [O] before RH decarburization.

With respect to the control of free oxygen after decarburization, as shown in Fig. 8, when the [O]/[C] mass ratio is less than 1.33 (theoretical value), forced decarburization mode is adopted. Under forced decarburization mode, the range of free oxygen content after decarburization is wide because of the fluctuation of oxygen blowing. If free oxygen after decarburization is controlled to be less than 400×10^{-6}, the [O]/[C] mass ratio in liquid steel before RH decarburization should be controlled to be between 1.5 and 2.0 and the carbon range should be 0.030wt% to 0.040wt% with natural decarburization.

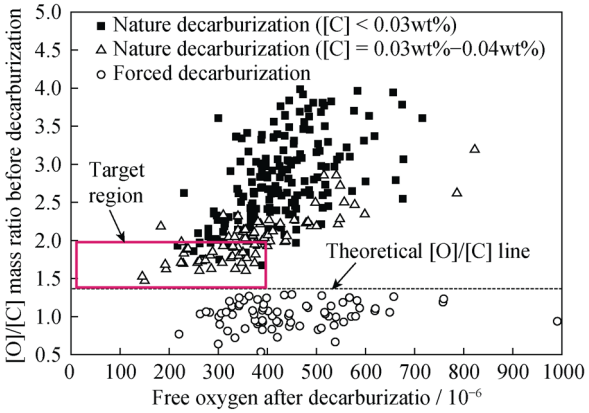

Fig. 8. Free oxygen after decarburization under different [O]/[C] mass ratios.

Fig. 9 explains how to ensure the exact range of carbon and free oxygen at the BOF endpoint on the basis of the RH

target region. When the [O]/[C] mass ratio is controlled between 1.5 and 2.5 at the BOF endpoint, 80% of the heats fall within the ideal control region for RH natural decarburization.

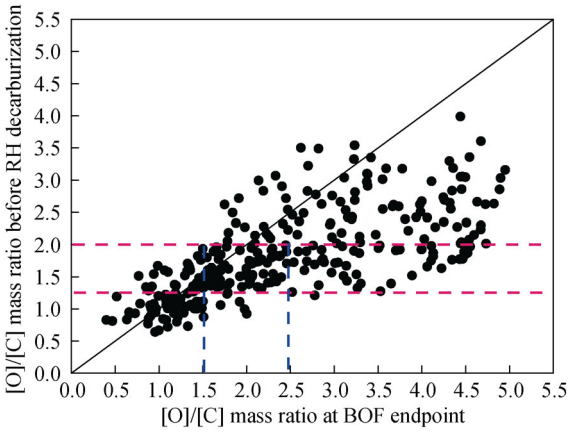

Fig. 9. Relationship between [O]/[C] mass ratio at the BOF endpoint and RH before decarburization.

On the basis of the aforementioned analysis, we derived the control ranges of [O] and [C] at the BOF endpoint. The free oxygen lower limit is 574×10^{-6}, and the upper limit is 775×10^{-6}; the carbon content lower limit is 297×10^{-6}, and the upper limit is 400×10^{-6}. The final target regions at different locations are listed in Table 5.

Table 5. Target region at different locations

Location	[O]/[C] mass ratio	[C] / 10^{-6}	[O] / 10^{-6}
BOF end point	1.5–2.5	297–400	574–775
RH before decarburization	1.5–2.0	300–400	500–700
RH after decarburization	—	< 20	< 400

To check the coordinated control relationship of target regions before and after RH decarburization, we conducted 23 heats for RH decarburization to verify the model in a 210-t ladle. Finally, the data for 14 heats with initial conditions before decarburization in target region A (see Fig. 10) were successfully obtained. Fig. 10 shows that the final carbon and residual oxygen in 85% of the heats were less than 15×10^{-6} and 400×10^{-6}, respectively, after RH natural decarburization under the initial conditions in region A, which is consistent with the previous analysis. When the carbon and oxygen before decarburization were in the range from 350×10^{-6} to 400×10^{-6} and from 500×10^{-6} to 650×10^{-6}, respectively, the residual oxygen after decarburization could be kept below 350×10^{-6}. In fact, when the initial conditions were outside the target region before decarburization, almost all of the heats' residual oxygen exceeded the final region B. High residual oxygen results in poor steel cleanness with the same removal time because more inclusions are formed after de-oxidation. Thus, coordinated control of the carbon and oxygen contents during RH was the key point for improving steel cleanness.

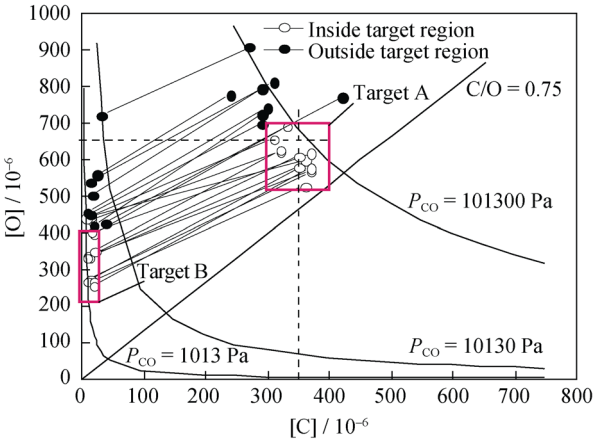

Fig. 10. Change of [C] and [O] during the RH decarburization process.

4. Conclusions

The coordinated control of carbon and oxygen contents can greatly reduce the generation of inclusions due to low free oxygen after decarburization, which is useful for clean steel production. We developed a strategy for the coordinated control of carbon and oxygen contents at the BOF endpoint and in the RH process on the basis of our analysis of the BOF and RH data for 489 heats. Reasonable conditions for controlling the carbon and oxygen contents are summarized as follows:

(1) The [C]·[O] product is stable in the range from 22×10^{-8} to 24×10^{-8} and is close to the equilibrium line at the BOF endpoint when the temperature is between 1695 and 1715°C and the furnace campaign is between 1000 and 5000 heats for BOF endpoint control.

(2) Maintaining an [O]/[C] mass ratio between 1.5 and 2.0 and a carbon range between 0.030wt% and 0.040wt% in liquid steel before RH decarburization satisfies the requirements of RH natural decarburization, and the free oxygen after decarburization can be controlled to be below 400×10^{-6}. To realize coordinated control of carbon and free oxygen, the carbon and free oxygen should be controlled to be between 297×10^{-6} and 400×10^{-6} and between 574×10^{-6} and 775×10^{-6}, respectively, at the BOF endpoint.

(3) Accuracy control of the BOF endpoint was achieved using the prediction formula $\eta = 1.52 + 132481.34 / \{1 +$

$\exp[(x+0.94)/0.11]\}$, which established a relationship between the temperature change per 0.01wt% reduction of carbon and the first-catch carbon in liquid steel in the BOF process.

Acknowledgements

This work was financially supported by the State Key Laboratory of Advanced Metallurgy Foundation in China (No. KF13-09), the National Natural Science Foundation of China (No. 51404018), the Fundamental Research Funds for the Central Universities (No. FRF-TP-14-125A2), and the Doctoral Fund of the Ministry of Education of China (No. 20130006110023).

References

[1] B. Deo, A. Overbosch, B. Snoeijer, D. Das, K. Srinivas, Control of slag formation, foaming, slopping, and chaos in BOF, *Trans. Indian Inst. Met*., 66(2013), No. 5, p. 543.

[2] B. Deo, A. Karamchetty, A. Paul, P. Singh, and R.P. Chhabra, Characterization of slag-metal droplet-gas emulsion in oxygen steelmaking converters, *ISIJ Int*., 36(1996), No. 6, p. 658.

[3] G.H. Li, B. Wang, Q. Liu, X.Z. Tian, and R. Zhu, A process model for BOF process based on bath mixing degree, *Int. J. Miner. Metall. Mater.*, 17(2010), No. 6, p. 715.

[4] P.H. Li, Y.P. Bao, F. Yue, and J. Huang, BOF end-point control of ultra low carbon steel, *Iron Steel*, 46(2011), No. 10, p. 27.

[5] Z.Z. Li, R. Zhu, R.Z. Liu, M. Lu, and H.Z. Wang, Effect of oxygen lance position on the flow velocity of molten steel in BOF, *J. Univer. Sci. Technol. Beijing*, 36(2014), Suppl. 1, p. 15.

[6] K.D. Schnelle and R.S.H. Mah, Production quality management using a real-time expert system, *ISIJ Int*., 34(1994), No. 10, p. 815.

[7] L. Liu, Converter control information and its on-line measurement (A), *Metall. Ind. Autom.*, 24(2000), No. 2, p. 5.

[8] K. Feng, H.B. Wang, A.J. Xu, and D.F. He, Endpoint temperature prediction of molten steel in RH using improved case-based reasoning, *Int. J. Miner. Metall. Mater.*, 20(2013), No. 12, p. 1148.

[9] P. Chen and Y.Z. Lu, Mimetic algorithms-based neural network learning for basic oxygen furnace endpoint prediction, *J. Zhejiang Univ. Sci. A*, 11(2010), No. 11, p. 841.

[10] M.X. Feng, Q. Li, and Z.S. Zou, A outlier identification and judgment method for an improved neural-network BOF forecasting model, *Steel Res. Int*., 79(2008), No. 5, p. 323.

[11] M. Kanemoto, H. Yamane, T. Yoshida, and H. Tottori, An application of expert system to LD converter processes, *ISIJ Int*., 30(1990), No. 2, p. 128.

[12] M.A. Ende, Y.M. Kim, M.K. Cho, J.H, Choi, and I.H. Jung, A kinetic model for the Ruhrstahl Heraeus (RH) degassing process, *Metall. Mater. Trans. B*, 42(2011), No. 3, p. 477.

[13] Y. Higuchi, H. Ikenaga, and Y. Shirota, Effects of [C], [O] and pressure on RH vacuum decarburization, *Tetsu-to-Hagnae*, 84(1998), No. 10, p. 21.

[14] Y.Q. Sun and Y.Z. Li, Thermodynamical evaluation of calculating formula for activity coefficient of iron oxide, *J. Baotou Univ. Iron Steel Technol.*, 20(2001), No. 3, p. 219.

[15] F.P. Tang, Z. Li, X.F. Wang, B.W. Chen, and P. Fei, Cleaning IF molten steel with dispersed *in-situ* hetero-phases induces by the composite sphere explosive reaction in RH ladles, *Int. J. Miner. Metall. Mater.*, 18(2011), No. 2, p. 144.

[16] B.S. Liu, G.S. Zhu, H.X. Li, B.H. Li, Y. Cui, and A.M. Cui, Decarburization rate of RH refining for ultra low carbon steel, *Int. J. Miner. Metall. Mater.*, 17(2010), No. 1, p. 22.

[17] J.M. Zhang, L. Liu, X.Y. Zhao, S.W. Lei, and Q.P. Dong, Mathematical model for decarburization process in RH refining process, *ISIJ Int*., 54(2014), No. 7, p. 1560.